SINERGI Vol. 26, No. 2, June 2022: 223-228
http://publikasi.mercubuana.ac.id/index.php/sinergi
http://doi.org/10.22441/sinergi.2022.2.011

An analysis of the effect of the bow entrance angle on ship resistance

S. Samuel[1], Sam Timoty Frans Evan S.[1], Andi Trimulyono[1], Muhammad Iqbal[2]
[1]Department of Naval Architecture, Faculty of Engineering, University of Diponegoro, Indonesia
[2]Department of Naval Architecture, Ocean, and Marine Engineer, University of Strathclyde, United Kingdom

Abstract
Modifying the hull shape is one of the challenges in designing a ship. The angle of the ship's entrance is a significant determinant of the total resistance of the ship. This research aimed to analyze the total resistance of the ship due to changes in the shape of the ship's bow. This research used the Computational Fluid Dynamics (CFD) method with overset mesh technique to predict the ship's total resistance and trim angle. Parameters used in the five-speed numerical simulations. This research indicated that a change in the bow angle of the ship results in a 5% change in the ship's resistance for every change in the bow entrance angle. Therefore, the prediction of total resistance shows significant results in planning conditions. Compared to another bow entrance angle at low Fr, total resistance has no noticeable differences. Angle changes of the entrance of the ship's bow also significantly affected the trim conditions on the ship according to the speed. At Fr 1.03, the stern trim angle tended to decrease dramatically. As a result, the trim by stern under porpoising probably oscillates considerably.

Keywords:
Ship's Bow;
Hull Entrance;
Drag Force;
CFD;

Article History:
Received: August 30, 2021
Revised: November 16, 2021
Accepted: December 10, 2021
Published: June 1, 2022

Corresponding Author:
S. Samuel
Naval Architecture Department, University of Diponegoro, Indonesia
Email: samuel@ft.undip.ac.id

INTRODUCTION

A planning hull ship is a ship that has more than one Froude Number (Fr). The high speed of a ship is directly related to the characteristics of the drag and shape of the hull. A planning hull ship is designed at speed and can be lifted to reduce frictional resistance and wave resistance [1]. High-speed ships cause a dynamic effect on the hull, namely trim. It happens because of the hydrodynamic characteristics of the hull geometry [2]. Planning hull ships are designed by taking into account their hydrodynamic characteristics. Modifying the hull's shape can improve the drag and maneuverability of the ship [3].

The modification or engineering of the hull shapes reduces the ship's resistance and the main propulsion energy of the ship, which will impact economic and technical factors when the ship is operating. The shape of the ship's bow is critical, especially the ship's speed [4]. The angle of entry (α) is the angle formed by the horizontal axis factor or the centerline, which is the longitudinal line of the ship with the ship's waterline when the ship is fully loaded [5].

Research conducted by Eko et al. regarding the hull entrance [6] showed that each modification of the angle of 3^0 changed the resistance by approximately 3.5%. Meanwhile, in Yu et al. [7], the optimal shape of the bulk carrier ship that did not use a bulbous bow reduced 13.2% wave resistance and 13.8% additional resistance. A numerical ventilation issue arises in numerical simulation research. Studies have been done to predict the overall drag of high-speed vessels [8].

Trim is a concept relating to ship dynamics at a high-speed vessel. It required a trim control device [9]. This research aimed to analyze the ship's resistance by engineering the bow angle on a planning type ship based on previous

research. Because changes in the trim angle significantly affected the total ship resistance, this research examined the trim angle's effect on the ship's resistance.

METHOD

Ship's Geometry

The research object was the planning hull ship. The analysis of this research aimed to predict the value of total resistance and trim. The main dimension of ships can be seen in Table 1.

Figure 1 was a ship in 3D as the initial design. The initial design of the ship used a bow entrance angle of 22^0. Changes in the ship's hull entrance were done by engineering the ship's lines plan on the draft. Figure 2 was a half breadth plan with a change in the ship's hull entrance of 3^0. By changing the angle of the bow entrance, the ship's volume displacement will change less than $6x10^{-4}$ %. The modified ship displacement value showed a similar value.

Hull Variation

The variation used in this research was based on the Lackenby method [10] with a curve relationship, namely Draft water line (DWL) and Sectional Area Curve (SAC), and implemented by [11].

Table 1. The main dimension

Parameter	Description
Scale	1 : 1
Type	Planning Hull
Length Overall	15.00 m
Length of Waterline	13.35 m
Length of Perpendicular	13.25 m
Breadth	4.00 m
Draft	0.76 m
Depth	2.13 m
Displacement	16.26 ton
Coefficient Block	0.41
Entrance Angle	22^0

Figure 1. Body Plan of Ship

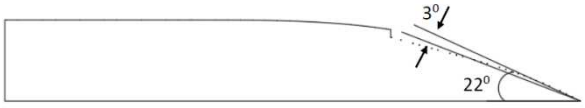

Figure 2. Half Breadth Plan View

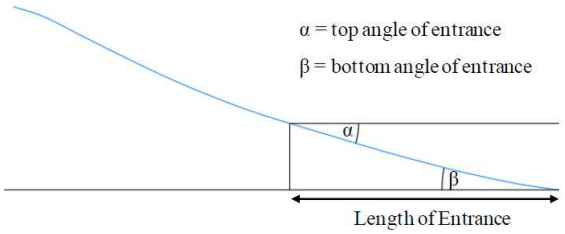

Figure 3. Variation of Hull Entrance

The parameter was done using the variables of α and β, as shown in Figure 3. This is because the values of α and β had the same value.

Ship modelling was done by making 2-D and 3-D models. The modelling used NURBS as a representation of the ship's geometry. NURBS is a mathematical model to help interface ship's geometry.

Computational Fluid Dynamics (CFD)

Computational Fluid Dynamics (CFD) is a computer-based fluid simulation. The two-phase flow of air and water is modelled using a Fully Eulerian formulation for fluid-structure-interaction. Problems involving immiscible fluid mixes and free surfaces are solved using the Volume of Fluid (VOF) multiphase model. The Dynamic Fluid Body Interaction (DFBI) module calculates a vessel's motion in response to forces. Heave and trim are set to be free, but roll and sway are fixed.

CFD solutions were used to calculate the resistance and dynamic pressure acting on the hull's surface. In the present research, the Reynolds-Averaged Navier-Stokes (RANS) equation is based on the conservation of mass and momentum in the fluid domain. Fluid was assumed to be two-phase and incompressible. The above momentum equation's Reynolds-averaged form, which includes turbulent shear forces, is given by:

$$\nabla \cdot V = 0 \tag{1}$$

$$\rho \frac{\partial V}{\partial t} = -\nabla P + \mu \Delta V + \nabla \cdot T_{Re} + S_M \tag{2}$$

Where ∇ is volume, V is an average velocity vector, ρ is density, P is the average compressive field, μ is dynamic viscosity, t is time, T_{Re} is a Reynolds stress tensor, Δ is displacement, and SM is a vector of momentum sources. According to the Boussinesq hypothesis, the T_{Re} component is calculated using the specified turbulence model:

$$\tau_{ij}^{Re} = \left(\frac{\partial V_i}{\partial x_j} + \frac{\partial V_j}{\partial x_i} \right) - \frac{2}{3} \rho k \delta_{ij} \tag{3}$$

where μ_t is the turbulent viscosity, k is the turbulent kinetic energy. The turbulence models can be used to cover hydrodynamic problems in the RANS method. The two equations turbulence model is widely used in hydrodynamics, such as SST k − ω and k − ε [12].

This research used an overset mesh to model the ship on the moving fluid problem. An offset grid is advantageous when dealing with fluid-structure interactions involving moving bodies. In the overset grid system, the overlapping mesh was used, and an overlapping grid block surrounding the planning hull was put on top of a background grid, which moves together with the ship's motion. Using an overset mesh involves the creation of one or more overset regions, which contain the physical bodies, and one or more background regions, which are closed surface solution domains. On top of the background region, more than one overset region can be employed. These overset sections may also be overlapping. This system works to find donor cells for each acceptor cell. The number of active cells in the donor zone around the acceptor cell centroid determines the number of donor cells, as shown in Figure 4. The overset mesh better captures the large motions of the planning hull at high Froude Numbers. However, the rigid body motion system is incompatible with substantial hull motions caused by flow misalignment [13][14].

This research referred to International Towing Tank Conference (ITTC) regulations to ensure accuracy in numerical calculations performed by the Star CCM+ code. The ITTC is an organization that is responsible for predictions about ship hydrodynamics based on the results of physical and numerical experiments. The recommendations used in calculating the ship resistance were as follows: (1) grid on the ship wall (y+); (2) time-step; (3) mesh-type; (4) the size of the fluid domain; and (5) grid density [15].

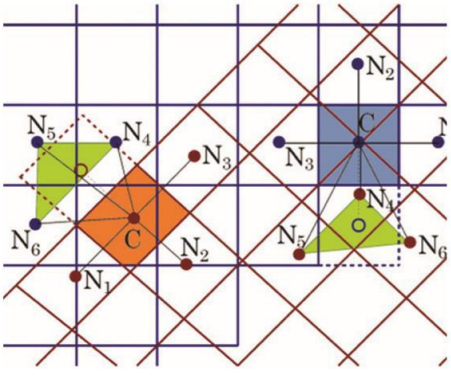

Figure 4. Overset Mesh System [16]

This research relied on Courant-Friedrichs-Lewy numbers (CFL) to determine the time step. The CFL number represented the number of points traversed by a fluid particle in a time interval. The faster the ship, the smaller the time-step that was used [16]. Therefore, this research calculated the time-step, which referred to the calculations recommended by ITTC as (4). In this study, the time step used was 0.005.

$$\Delta t\ ITTC = 0.005 \sim 0.01 L/U \quad (4)$$

The sizes used in the overset mesh are described in Table 2. The overset mesh Interface is used to couple the overset regions with the background region. As a background, the vessel's stern is placed at the longitudinal position of zero. The water depth has been set to be 1.9L. However, the overset region is set to be 0.75H. Figure 5 shows the dimensions of the fluid domain following the ITTC recommendations [17]. The length of the ship L, the height of the ship H, and the width of the ship B.

The highest concentration of mesh was located on the hull and water surface. It aimed to reduce the simulation time. CFD simulation was carried out using a half-body ship. It also aimed to reduce the simulation time.

Before presenting the results, the computational approach was put to the test by completing a numerical convergence analysis for the overset grid system. Validation with a benchmark Fridsma hull has been done. When using the overset grid system as described in [8], five different grid types were used to perform CFD verification, which are 0.48 M, 0.89 M, 1.44 M, 2.33 M, and 2.99 M. The number of cells 2.3 M and 2.99 M show convergence results, according to numerical simulation analyses.

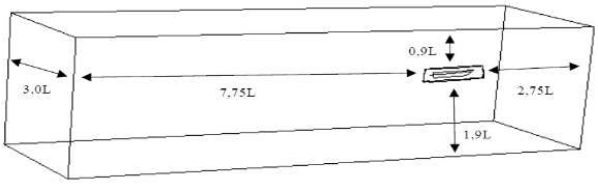

Figure 5. Fluid domain

Table 2. Towing Tank Size

Parameter	Background	Overset
Length (m)	7.75L from FP	0.25L of FP
	2.75L from AP	0.25 of AP
Height (m)	0.9L from top	0.75H of top
	1.9L from bottom	0.75H of bottom
Width (m)	3L of symmetry	0.5B of symmetry

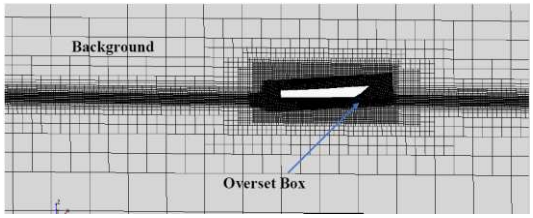

Figure 6. Overset Mesh

However, the number of grid mesh 2.99 M requires more time to complete simulations than 2.3 M. As a result, grid mesh 2.3 M was used for the rest of the CFD simulations. There was good agreement between the numerical estimate and the experiment in this investigation, with approximately 11.2 percent of the differences. Figure 6 shows the overset mesh.

RESULTS AND DISCUSSION

Numerical analysis tests were carried out at five-speed to predict the ship's drag characteristics. This research will concentrate on planning circumstances, as the primary goal of this ship is to be employed at high speeds. The two-phase flow consisting of air and water was solved using the VOF method, which follows the free surface boundary. The DFBI model provided two degrees of freedom (DOF) for the hull. The planning vessel was allowed to heave and trim.

Figure 7 presents the analysis of the total resistance of the ship. The components of the total ship resistance consisted of two, namely residual resistance and frictional resistance.

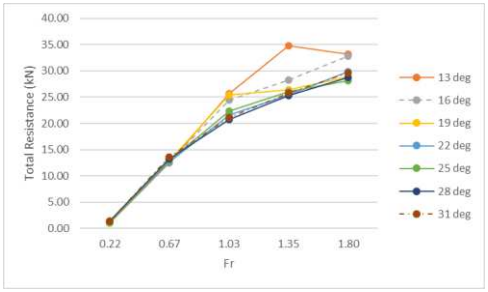

Figure 7. Total Resistance

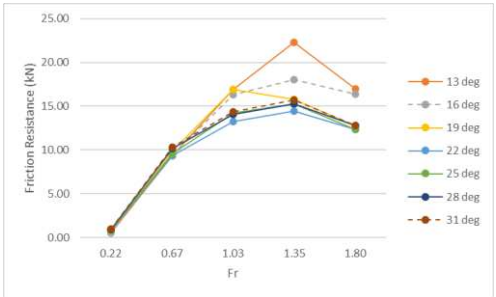

Figure 8. Friction Resistance

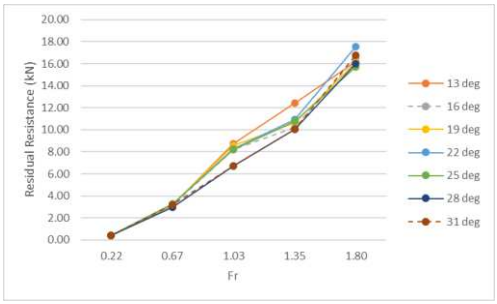

Figure 9. Residual Resistance

Figure 8 shows the result of the ship's frictional resistance analysis. Figure 9 shows the result of the analysis of residual resistance on the ship. For displacement type, frictional resistance is more dominant than residual resistance. It happened because it was related to the ship's WSA. Consequently, the frictional stress on the hull generally will increase along with the ship. There are two types of pressure to which the vessel is subjected: hydrostatic and hydrodynamic pressure. The buoyancy force is proportional to the ship's submerged volume (displacement) and is determined by hydrostatic pressure. The hydrodynamic pressure is proportional to the square of the ship speed and is determined by the flow around the hull. A form resistance component exists because of the interaction between the ship's shape and viscosity. The form resistance effect showed three parameters: frictional, viscous, and flow separation.

The analysis results carried out in Figure 7 showed an increasing trend in ship resistance. The greater the ship's Froude Number, so the more excellent the total ship resistance is. It applied to residual and frictional resistance, which were components of the total drag of the ship.

Figure 7 at Fr < 0.67 was called the displacement mode condition, the analysis results showed that the bow entrance angle of 13^0 had the smallest total resistance value in these conditions. However, compared with another bow entrance angle at low Fr does not show significant resistance differences. While at Fr > 1 or planning mode conditions, the angle of 22^0 until 31^0 indicated a smaller total resistance value. This condition shows a similar total resistance on several Froude Numbers. The difference is caused by the interaction of the entrance angle with the spray, which only occurs at high speeds.

The force and the resulting moment acting on the body are obtained by the fluid pressure (residual resistance) and shear forces (friction resistance) acting on each face of the body's

boundaries. The DFBI model represents the motion of a rigid body in response to the fluid's pressure and shear forces on the body. The algorithm estimates the total force and moment acting on the body due to all influences, then solves the rigid body motion governing equations to get the rigid body's new location relative to the body's local coordinate system. Another reason was that the planning hull-type ship had a high speed, so the trim by stern that occurred affected the total resistance value.

In the Savitsky approach, several factors can affect the value of ship resistance, namely ship speed, WSA (Wetted Surface Area), and ship trim value [18][19]. Ship speed and WSA had a value that was directly proportional to the value of the ship's resistance, while the trim value of the ship was inversely proportional to the total resistance value of the ship.

At Fr < 1, reducing the bow entrance angle could reduce the total drag. Meanwhile, at Fr > 1, increasing the ship's hull entrance angle could reduce the total ship's resistance due to the planning condition.

Figure 10 shows the volume fraction of water as the definition of water and air. The properties of the meshing were shown in red and blue. The value 0 was the air fraction, and the value 1 was the water fraction. Figure 11 was the result of the WSA analysis which showed the area of the hull submerged in water. Displacement and WSA values were directly proportional to the total resistance of the ship. Therefore, WSA was very influential on the frictional resistance of the ship. The greater the WSA, the greater the value of the frictional resistance of the ship.

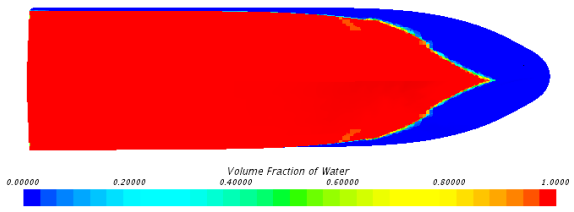

Figure 10. Wetted Surface Area (WSA)

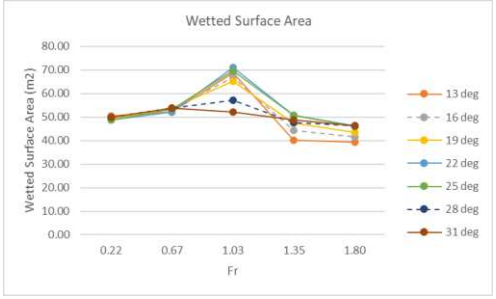

Figure 11. Volume Fraction of Water on Fr 1.35

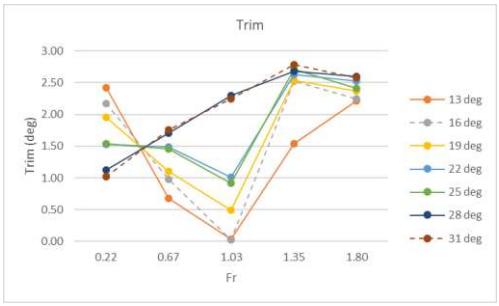

Figure 12. Trim Angle

The ship's bow angle engineering could improve the ship's trim condition at a certain speed. At Fr 0.22, there was a decrease in the trim angle of the ship along with the change in the angle of the bow (hull entrance), while at Fr 0.67, there was an increase in the trim angle of the ship along with the change in the angle of the bow of the ship. There was a change in the trim value of the ship due to the difference in the centre of gravity of each ship model with a different bow angle.

From the analysis carried out on the planning hull, the trim condition can be improved by engineering the hull entrance according to the speed shown in Figure 12. At Fr 0.22, the smallest trim angle was 31^0. The trim value can be improved by increasing the bow entry angle. While at Fr ≥ 0.67, the smallest trim angle was at an angle of 13^0, meaning that the trim value could be improved by reducing the bow angle of the ship. The angle of trim by stern tended to decrease significantly at FR 1.03. Thus, the trim by stern under porpoising oscillates largely, as shown in Figure 12. To prevent the porpoising phenomenon, it is effective to add appendages at the stern to generate many bow-down moments, as we know, interceptor and trim tab. The trim condition of the ship had a significant effect on the total resistance value of the ship. The more increase the trim angle value of the ship or the smaller the wet area or Wetted Surface Area (WSA), the smaller the value of the total resistance of the ship.

CONCLUSION

It was found that the change in the hull entrance of the ship by 3^0 can significantly affect the total ship resistance. Modifying the ship's bow had a total drag effect of 5%. Significant results occurred at Fr < 1, where the smaller the bow angle of the ship, the smaller the value of the ship's resistance. Meanwhile, for Fr > 1, the greater the bow angle of the ship, the smaller the ship's resistance. It happened because the factors that significantly affected the value of the ship's resistance were speed, WSA, and ship trim

angle. Following the approach taken by Savitsky, the value of speed and WSA was directly proportional to the value of the total resistance of the ship. The value of the trim angle of the ship was inversely proportional to the value of the total resistance of the ship. These changes improved the trim condition of the ship according to the speed of the ship.

REFERENCES

[1] G. Hou, B. Johnson, J. Degroff, S. Trenor, and J. Michaeli, "Dynamic response modeling of high-speed planing craft with enforced acceleration," *Ocean Engineering*, vol. 192, p. 106493, 2019, doi: 10.1016/ j.oceaneng.2019.106493.

[2] A. G. Avci and B. Barlas, "An experimental and numerical study of a high speed planing craft with full-scale validation," *Journal of Marine Science and Technology,* vol. 26, no. 5, pp. 617–628, 2018, doi: 10.6119/JMST. 201810_26(5).0001.

[3] D. J. Kim, K. P. Rhee, Y. G. Kim, S. Y. Kim, S. H. Kim, and Y. J. You, "Design of high-speed planing hulls for the improvement of resistance and seakeeping performance," *International Journal of Naval Architecture and Ocean Engineering*., vol. 5, no. 1, pp. 161–177, 2013, doi: 10.2478/ijnaoe-2013-0124.

[4] D. Chrismianto, A. Trimulyono, and M. N. Hidayat, "Analisa Pengaruh Modifikasi Bentuk Haluan Kapal Terhadap Hambatan Total dengan Menggunakan CFD," vol. 11, *KAPAL,* no. 1, pp. 40–48, 2014, doi: 10.12777/ kpl.11.1.40-48.

[5] H. A. Luhur P, E. S. Hadi, and W. Amiruddin, "Analisa Pengaruh Sudut Masuk Kapal Perintis 750 DWT terhadap Resistance Kapal dengan Menggunakan CFD," *Jurnal Teknik Perkapalan*, vol. 5, no. 2, pp. 421–430, 2017.

[6] E. S. Hadi, P. Manik, and M. Iqbal, "Influence of hull entrance angle 'perintis 750 DWT', toward ship resistance: The case study for design development 'perintis 750 DWT.,'" *MATEC Web Conference*, vol. 159, pp. 2–7, 2018, doi: 10.1051/matecconf/ 201815901057.

[7] J. W. Yu, C. M. Lee, I. Lee, and J. E. Choi, "Bow Hull-Form Optimization in Waves of a 66,000 DWT Bulk Carrier," *International Journal of Naval Architecture and Ocean Engineering*, vol. 9, no. 5, pp. 499–508, 2017, doi: 10.1016/j.ijnaoe. 2017.01.006.

[8] S. Samuel, D. J. Kim, A. Fathuddiin, and A. F. Zakki, "A Numerical Ventilation Problem on Fridsma Hull Form Using an Overset Grid System," *IOP Conference Series: Materials Science and Engineering*, vol. 1096, no. 1, p. 012041, 2021, doi: 10.1088/1757-899x/1096/1/012041.

[9] C. Judge *et al*., "Experiments and CFD of a High-Speed Deep-V Planing Hull—Part I: Calm water," *Applied Ocean Research*, vol. 96, pp. 102–060, 2020, doi: 10.1016/j.apor. 2020.102060.

[10] H. Lackenby, "On The Systematic Variation of Ship Forms," *Transaction of Instrumentation of Naval Architecture*, vol. 92, pp. 289–316, 1950.

[11] M. Iqbal and S. Samuel, "Traditional catamaran hull form configurations that reduce total resistance," *International Journal of Technology*, vol. 8, no. 1, pp. 85–91, 2017.

[12] J. E. Bardina, P. G. Huang, and T. J. Coakley, "Turbulence modeling validation, testing, and development," *Research Report*, Ames Research Center, California, 1997.

[13] O. F. Sukas, O. K. Kinaci, F. Cakici, and M. K. Gokce, "Hydrodynamic assessment of planing hulls using overset grids," *Applied Ocean Research*, vol. 65, pp. 35–46, 2017, doi: 10.1016/j.apor.2017.03.015.

[14] O. Yendri, "Effect of Water on Flow Fluctuation in River Flow," *Journal of Integrated and Advanced Engineering (JIAE)*, vol. 2, no. 1, pp. 1-10, 2022, doi: 10.51662/jiae.v2i1.23

[15] NN, "Recommended Procedures and Guidelines Practical Guidelines for Ship CFD," *ITTC*, no. 9, pp. 1–18, 2011.

[16] NN, "User guide STAR-CCM 13.02.011-R8," *CD-Adapco*, 2017.

[17] S. Samuel, S. Jokosisworo, M. Iqbal, P. Manik, and G. Rindo, "Verifikasi Deep-V Planing Hull Menggunakan Finite Volume Method Pada Kondisi Air Tenang," *Teknik*, vol. 41, no. 2, pp. 126–133, 2020, doi: 10.14710/teknik.v0i0.29391.

[18] R. Khazaee, M. A. Rahmansetayesh, and S. Hajizadeh, "Hydrodynamic evaluation of a planing hull in calm water using RANS and Savitsky's method," *Ocean Engineering*, vol. 187, no. July, p. 106221, 2019, doi: 10.1016/ j.oceaneng.2019.106221.

[19] B. Metheny, R. Permatasari, M. S. Annas, "Design modeling of savonius-darrieus turbine for sea current electric power plant," *SINERGI,* vol. 25, no. 1, pp. 27-32, 2021, doi: 10.22441/sinergi.2021.1.004